Methods for analyzing spectroscopic line shapes. NMR solid powder patterns

D. W. Alderman, Mark S. Solum, and David M. Grant

Citation: J. Chem. Phys. **84**, 3717 (1986); doi: 10.1063/1.450211
View online: http://dx.doi.org/10.1063/1.450211
View Table of Contents: http://jcp.aip.org/resource/1/JCPSA6/v84/i7
Published by the American Institute of Physics.

Methods for analyzing spectroscopic line shapes. NMR solid powder patterns

D. W. Alderman, Mark S. Solum, and David M. Grant
Department of Chemistry, University of Utah, Salt Lake City, Utah 84112

(Received 23 October 1985; accepted 26 December 1985)

A new method is described for numerically computing theoretical NMR powder patterns which achieves a many-fold increase in speed and accuracy over previous techniques. The method incorporates a simple and efficient technique for selecting the set of crystal orientations over which the spectral frequencies are calculated. The orientation selection technique is then integrated with an interpolation scheme which transfers the intensities at these frequencies to the computed spectrum. The method will be useful whenever an average over a sphere is computed numerically. The new efficiency of the method makes practical least squares fitting of theoretical spectra to experimental NMR data. The fits provide unbiased estimates of the NMR parameters and their errors. The technique is illustrated by extracting chemical shift tensors from a proton decoupled carbon-13 NMR spectrum.

INTRODUCTION

NMR spectra from dilute nuclei in powdered solids exhibit broad bands which result from the superposition of signals from the randomly oriented single crystals.[1-6] Such powder spectra often have characteristic band shapes with well defined features such as peaks, breaks, and shoulders. In simple cases analytic solutions exist[1,7] and it is possible to read the NMR parameters directly from the spectrum. For example, in the case of a single isolated nucleus subject to an anisotropic chemical shift, the three principal values of the chemical shift tensor can be obtained directly from the frequencies of the two shoulders and the peak in the spectrum.[3,6] In more complicated instances, when a number of interactions, such as an anisotropic chemical shift and dipole–dipole coupling, are simultaneously present,[8] it is impossible to obtain all of the NMR parameters directly from the spectra because analytical expressions for the powder band shape do not exist. Instead it is necessary to compute numerically the powder spectrum using various values of the NMR parameters, and then to adopt as correct those values for which the computed spectrum most closely resembles the experimental spectrum.[8,9]

COMPUTATION OF POWDER SPECTRA

A powder spectrum is computed by summing the spectra from an ensemble of randomly oriented single crystals. Previous techniques for summing[6,8-11] consist in producing a histogram by uniformly dividing the spectral width in which the spectrum lies into a large number of bins, each corresponding to a small frequency interval. Then for each of many orientations, the frequency and intensity of each line in the single crystal spectrum is calculated. The number representing the intensity of each line is then added to the bin whose frequency interval contains the frequency of the line. After all orientations are accounted for, the resulting histogram is an approximation of the powder spectrum. The finer the division of the frequency interval and the more orientations used, the better the approximation.

When viewed from the laboratory frame of reference, where the magnetic field is fixed, the requirement is to sum over all possible crystal orientations, which would imply summing over three variables such as the Euler angles. But by working in a frame of reference attached to the crystal, the sum can be done over all directions of the magnetic field, which is specified by two quantities, e.g., the polar angles.

Because all orientations of the crystals are equally likely, the summation of spectra must correspond to a uniform distribution of the magnetic field over all directions. In fact the inversion symmetry of the magnetic interactions assures that the single crystal spectrum is the same for two oppositely directed magnetic field vectors. It is thus necessary to cover only half of all directions to obtain the correct result. If higher symmetry is present, the calculation can be further truncated.[5]

Since there is no simple way to partition a sphere into a large number of spherical polygons of equal solid angle, it is impractical to define a finite set of magnetic field directions which accurately approximate the uniform distribution. It is thus necessary to choose a set of magnetic field directions and associate with each a weighting factor, proportional to the solid angle allotted to it, by which the intensity of the single crystal spectrum is scaled before being added to the sum, so as to obtain equal contributions from each unit of solid angle.

Previously powder patterns have been calculated by defining directions with the polar angle θ and the azimuthal angle ϕ and then stepping θ from 0° to 90° and ϕ from 0° to 360° through equal intervals on a mesh as fine as 1°.[6,8,10,11] The weighting factor is then $\sin(\theta)$. The problem with this approach is that the weighting factors are of widely differing values, so that while some calculations produce large contributions, others count only very little towards the result. When the time necessary to calculate each single crystal spectrum is significant, the total time for the calculation is quite large. If, in an effort to reduce the calculation time, a coarser mesh is chosen, the degree of approximation to the actual powder pattern may become unsatisfactory.

A simple scheme for partitioning all directions in which the weighting functions take on a more limited range of values can thus increase the efficiency of the calculation by producing a result of equal accuracy with fewer computations.

 0021-9606/86/073717-09$02.10

The calculation can be further improved by incorporating an interpolation scheme which, instead of adding intensity to only one bin in the spectrum, properly adds intensity to all bins which lay between the ones containing the frequencies of adjoining magnetic field orientations. Also, because the calculation of trigonometric functions is time consuming in a computer, a scheme which minimizes the frequency of this operation is preferred.

The method described below meets all of these criteria. It incorporates a simple yet effective interpolation scheme, partitions all directions into intervals of roughly equal solid angle, and produces the weighting function and the three direction cosines for each magnetic field orientation directly.

One-dimensional interpolation

For the purpose of illustrating methods of computing powder spectra, consider first an imaginary situation in which there is a single variable which describes the crystal orientation. For simplicity assume that the spectrum at any particular orientation consists of a single line whose intensity is independent of the orientation.

Figure 1(a) shows a hypothetical relation between resonant frequency f and a single orientation variable α. Figure 1(b) illustrates the α axis divided into a number of equally spaced points and the frequency calculated at each point.

The simplest way to calculate a powder spectrum is to divide the frequency axis into equal intervals, also shown in Fig. 1(b), count the number of calculated frequency points which lie in each interval, and display these counts on a histogram as in Fig. 1(c). In regions where the frequency as a function of α is changing rapidly, this method produces a rather jagged approximation of the spectrum, because when points adjacent in α produce frequencies which lie in nonadjacent bins, no intensity is added to the bins which have been skipped over. This method approximates the spectrum by sampling the range of the orientation variable α at discrete points and transferring the frequencies obtained at these points to the spectrum.

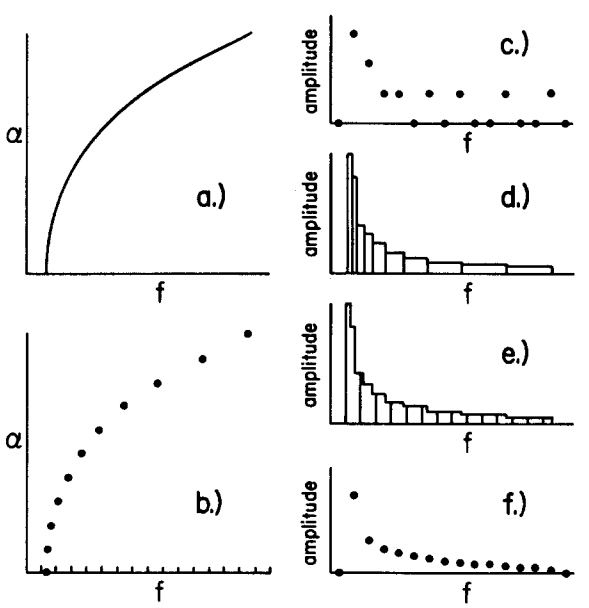

FIG. 1. (a) Frequency f as a function of a single orientational variable α. (b) Frequency calculated at uniform intervals in α. Frequency axis also divided into uniform intervals. (c) Histogram of the number of points which lie in each interval on the frequency axis. (d) Rectangles of constant area erected between the frequencies calculated at uniform increments in α. (e) Outline of rectangles divided at the uniform intervals in the frequency axis. (f) Areas of the rectangles in each frequency axis interval.

The interpolation scheme used here instead focuses on the intervals between the points at which the frequencies are calculated. Consider two adjacent points α_1 and α_2 at which the frequencies are f_1 and f_2. If the frequency as a function of α curve is approximated as a straight line between the points, the contribution to the spectrum from this orientation interval is a rectangle extending between the frequencies f_1 and f_2. To make the area of the rectangle unity its height is made the reciprocal of the absolute frequency difference, $1/|f_1 - f_2|$. The sum of the rectangles corresponding to all orientation intervals, such as in Fig. 1(d), is then an approximation of the spectrum from the whole range of α's. Since a discrete representation of the spectrum is ultimately necessary, the frequency axis is now divided into equal intervals as in Fig. 1(e), and the areas of the rectangles which lie over each interval computed. This result, shown in Fig. 1(f), is then the discrete representation of the spectrum. Because this interpolation method fills in intensity between the calculated frequencies, it produces a much smoother approximation in regions where the frequency as a function of α is changing rapidly.

When the intensity of the single crystal line is no longer constant but also a function of the orientation variable α, each rectangle can be adjusted to reflect the intensity by making its area the average of the two intensities at either end of the orientation interval.

When there is more than one line in each single crystal spectrum it is necessary only to calculate the powder spectrum which would result from each line, then add the results together.

Two-dimensional interpolation

The above interpolation method generalizes immediately to two dimensions. The single orientation parameter α now becomes two such parameters, α and β. The interval on the α line corresponds to an area in the α–β plane. Just as two points determine an interval in one dimension, three points at the vertices of a triangle are the simplest means by which an interval can be defined in two dimensions. The α–β plane partitioned into such intervals, and the three frequencies, f_1, f_2, and f_3 computed at the vertices of one interval, is illustrated in Fig. 2(a). It is convenient to sort the frequencies in ascending order and label them $f_{\min}$, f_{mid}, and $f_{\max}$. The frequency function can again be linearly interpolated, now by approximating the actual function by a plane passing through the three points. The contours of this plane within the interval are illustrated in Fig. 2(b) for the case where $f_{\min} = f_1$, $f_{\mathrm{mid}} = f_2$, and $f_{\max} = f_3$. The spectrum from those single crystals in the triangular orientation interval lies entirely between frequencies $f_{\min}$ and $f_{\max}$. Its intensity at a given frequency is proportional to the length of the contour at that frequency. The spectrum is thus the triangular "tent," illustrated in Fig. 2(c), whose edges lie at the lowest

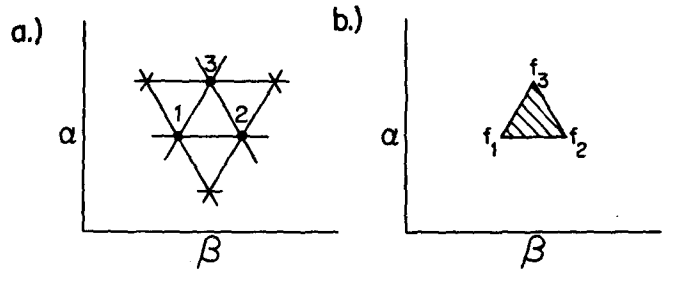

FIG. 2. (a) Two-dimensional space partitioned into a triangular grid. Three points at the vertices of a single triangle are labeled. (b) Contours of constant frequency for a linear interpolation between the three frequencies f_1, f_2, and f_3 at the vertices of the labeled triangle. (c) Tent corresponding to the spectrum from points within the labeled triangle.

and highest frequencies, f_{min} and f_{max}, and whose peak lies at the intermediate frequency, f_{mid}. In order for the tent to have unit area its peak height should be made $2/(f_{max}-f_{min})$. This result is independent of the shape of the orientation interval triangle.

The powder pattern spectrum is then obtained in the same way as in the one-dimensional case by summing the tents corresponding to the spectra from a set of triangular orientation intervals which cover the two-dimensional orientation space.

The discrete representation of the spectrum is again obtained by dividing the frequency axis into small intervals and computing the contribution of the tent spectrum in each interval. An interval is defined by its low limit, f_{low}, and its high limit, f_{high}. By convention an interval contains its low limit, f_{low}, but not its high limit, f_{high}, which is contained in the next interval. That part of the area of a tent which lies within a given interval depends upon five frequencies: those which define the interval, f_{low} and f_{high}, and those associated with the tent, f_{min}, f_{mid}, and f_{max}. A tent can be quite narrow, so that all of its area falls within a single interval, or it can be broad, extending into a number of frequency intervals, each of which must receive a fraction of the tent's area. Depending upon how a frequency interval lies relative to the tent, there are ten distinct cases. All cases can be calculated with the following equations for the fraction of the area of a tent which lies in an interval:

(a) $f_{low} \leqslant f_{min}, f_{max} < f_{high}$; interval contains f_{min}, f_{mid}, and f_{max}:

$$\text{Area} = 1. \tag{1a}$$

(b) $f_{high} \leqslant f_{min}$; entire interval lies at frequencies below those of tent, and thus interval contains neither f_{min}, f_{mid}, nor f_{max}:

$$\text{Area} = 0. \tag{1b}$$

(c) $f_{low} \leqslant f_{min} < f_{high} \leqslant f_{mid}$; interval contains f_{min} but not f_{mid}, and thus not f_{max}:

$$\text{Area} = \frac{(f_{high}-f_{min})^2}{(f_{max}-f_{min})(f_{mid}-f_{min})}. \tag{1c}$$

(d) $f_{min} < f_{low}, f_{high} \leqslant f_{mid}$; interval lies between f_{min} and f_{mid}:

$$\text{Area} = \frac{(f_{high}-f_{low})(f_{high}+f_{low}-2f_{min})}{(f_{max}-f_{min})(f_{mid}-f_{min})}. \tag{1d}$$

(e) $f_{low} \leqslant f_{min}, f_{mid} < f_{high} \leqslant f_{max}$; interval contains both f_{min} and f_{mid}, but not f_{max}:

$$\text{Area} = \frac{(f_{mid}-f_{min})}{(f_{max}-f_{min})} + \frac{(f_{high}-f_{mid})(2f_{max}-f_{high}-f_{mid})}{(f_{max}-f_{min})(f_{max}-f_{mid})}. \tag{1e}$$

(f) $f_{min} < f_{low} \leqslant f_{mid} < f_{high} \leqslant f_{max}$; interval contains f_{mid}, but neither f_{min} nor f_{max}:

$$\text{Area} = \frac{(f_{mid}-f_{low})(f_{mid}+f_{low}-2f_{min})}{(f_{max}-f_{min})(f_{mid}-f_{min})} + \frac{(f_{high}-f_{mid})(2f_{max}-f_{high}-f_{mid})}{(f_{max}-f_{min})(f_{max}-f_{mid})}. \tag{1f}$$

(g) $f_{min} < f_{low} \leqslant f_{mid}, f_{max} < f_{high}$; interval contains both f_{mid} and f_{max}, but not f_{min}:

$$\text{Area} = \frac{(f_{mid}-f_{low})(f_{mid}+f_{low}-2f_{min})}{(f_{max}-f_{min})(f_{mid}-f_{min})} + \frac{(f_{max}-f_{mid})}{(f_{max}-f_{min})}. \tag{1g}$$

(h) $f_{mid} < f_{low}, f_{high} \leqslant f_{max}$; interval lies between f_{mid} and f_{max}:

$$\text{Area} = \frac{(f_{high}-f_{low})(2f_{max}-f_{high}-f_{low})}{(f_{max}-f_{min})(f_{max}-f_{mid})}. \tag{1h}$$

(i) $f_{mid} < f_{low} \leqslant f_{max} < f_{high}$; interval contains f_{max}, but not f_{mid}, and thus not f_{min}:

$$\text{Area} = \frac{(f_{max}-f_{low})^2}{(f_{max}-f_{min})(f_{max}-f_{mid})}. \tag{1i}$$

(j) $f_{max} < f_{low}$; entire interval lies at frequencies above those of tent, and thus interval contains neither f_{min}, f_{mid}, nor f_{max}:

$$\text{Area} = 0. \tag{1j}$$

When the intensity of the spectrum is a function of the orientation, the area of each tent is made proportional to the average of the three intensities at the vertices of the triangular orientation interval.

Again, multiple lines in the single crystal spectrum are accommodated by adding the resultant powder spectra for each line.

Note the importance of partitioning the two-dimensional orientation space into triangular intervals. Since three points in space determine a plane, a triangular interval makes possible the linear interpolation of the frequency

function. If a four sided figure such as a square was used, it would in general be necessary to interpolate using a curved surface which passed through all four points.

Partitioning all directions

Partitioning all directions consists in selecting a set of orientation intervals in which to compute the single crystal spectra which are summed together to produce the powder pattern. The intervals should be defined by small triangles so that the two-dimensional interpolation scheme described above can be used, and they should all be of comparable solid angle so that the efficiency of the powder pattern calculation is high.

In order to derive an orderly triangular grid consider the octahedron of Fig. 3(a) placed so that its 6 vertices lie along the coordinate axes, its 8 faces lie in the octants defined by the signs of the three coordinates, and its 12 edges lie in the planes defined by one of the three coordinates being zero. If the octahedron is scaled such that its vertices all lie unit distance from the origin, the equation of the plane of its face which lies in the $x>0$, $y>0$, $z>0$ octant is simply $x+y+z=1$. The equations of the faces in the seven other octants differ only in the signs of the x, y, and z terms.

The equilateral triangle faces of the octahedron can now be partitioned in a particularly simple way. Figure 3(b) shows equally spaced contours of constant x, at $x=i/N$, where $N=4$ and $0\leqslant i\leqslant N$, ruled on the $x>0, y>0, z>0$ octant face and, similar contours of constant y at $y=j/N$ and constant z at $z=k/N$. These contours combined form a grid of N^2 equilateral triangles on the octahedron face. Now clearly every intersection of the grid is defined by its x and y coordinates, since the z coordinate can always be obtained from the equation $x+y+z=1$. Thus the intersections can be indexed with the integers i and j with $i\geqslant 0$, $j\geqslant 0$, and $i+j\leqslant N$. The index associated with the z coordinate is then given by $k=N-i-j$. The distance from the origin to the grid intersections is given by

$$R=(x^2+y^2+z^2)^{1/2}=(i^2+j^2+k^2)^{1/2}/N$$
$$=[i^2+j^2+(N-i-j)^2]^{1/2}/N. \tag{2}$$

The direction cosines describing the vector from the origin to the grid intersections are given by

$$l=\cos(\gamma_x)=x/R=i/[i^2+j^2+(N-i-j)^2]^{1/2}, \tag{3a}$$

$$m=\cos(\gamma_y)=y/R=j/[i^2+j^2+(N-i-j)^2]^{1/2}, \tag{3b}$$

$$n=\cos(\gamma_z)=z/R=(N-i-j)/[i^2+j^2+(N-i-j)^2]^{1/2}. \tag{3c}$$

Note that the direction cosines are obtained directly from the indices i and j, without recourse to time consuming trigonometric function evaluation. The direction cosines are often the most useful form in which to express the magnetic field direction. For example, the chemical shift at any magnetic field direction is given by the quadratic form

$$\delta=(lmn)\begin{pmatrix}\delta_{xx}&\delta_{xy}&\delta_{xz}\\ \delta_{yx}&\delta_{yy}&\delta_{yz}\\ \delta_{zx}&\delta_{zy}&\delta_{zz}\end{pmatrix}\begin{pmatrix}l\\ m\\ n\end{pmatrix}. \tag{4}$$

If trigonometric functions of the polar angles are required they can be obtained from the formulas.

$$\cos(\theta)=n, \tag{5a}$$

$$\sin(\theta)=(1-n^2)^{1/2}=(l^2+m^2)^{1/2}, \tag{5b}$$

$$\cos(\phi)=l/\sin(\theta), \tag{5c}$$

$$\sin(\phi)=m/\sin(\theta). \tag{5d}$$

The planar triangles ruled on four faces of the octahedron are a suitable set for the calculation of the single crystal spectra to be summed into the powder pattern. If the grid is fine enough so that the triangles are small, the two-dimensional linear interpolation method described above can be used to compute the spectrum associated with all magnetic field orientations which pass through each triangle.

Though the plane triangles on the faces of the octahedron all have the same area, they do not all subtend the same solid angle, and thus it is necessary to compute a weighting factor for each. The exact expression for the solid angle is quite complicated, but an excellent approximation which is correct in the limit of triangles whose edges are small compared to their distance from the origin is easy to obtain. The plane triangles subtend various solid angles because of two effects. First, their distance from the origin varies, and second, they are tilted so they are not viewed normally. The effect of the variation of the distance from the origin is given by the familiar inverse square law, which states that the solid angle subtended is proportional to $1/R'^2$, where R' is the distance from the origin to the plane triangle. The solid angle of the triangles is also reduced by the cosine of the angle between the normal to their plane and the direction from which they are viewed. Since the faces of the octahedron are at a distance $d=1/\sqrt{3}$ from the origin, this cosine is given by $d/R'=1/(\sqrt{3}R')$. Thus the total solid angle weighting factor for small triangles is equal to C/R'^3, where C is an constant into which the factors in the inverse square law and the viewing angle cosine have been absorbed. Because there is no single distance from the origin to a plane triangle, the factor C/R'^3 must be approximated. The average of C/R^3 at the three vertices, which can be calculated with Eq. (2), could

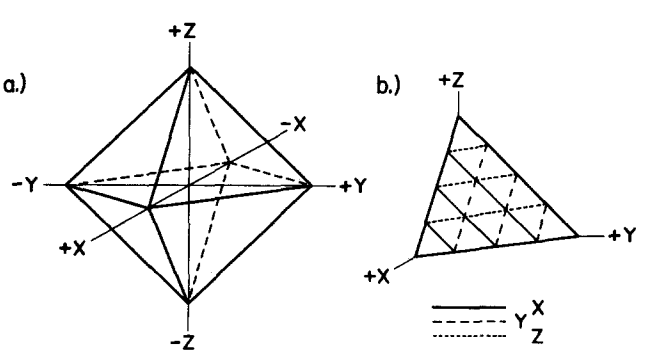

FIG. 3. (a) Octahedron with its center at the origin of a coordinate system and its vertices along the coordinate axes. (b) Face of the octahedron in the $x>0$, $y>0$, $z>0$ octant with lines of constant x (solid line), constant y (dashed line), and constant z (dotted line).

be used. But there is another factor, the intensity of the line in the single crystal spectra, which must also be included in the computation of the area of the spectrum tent corresponding to a particular triangle. This second factor is also calculated at the vertices of the triangles and it is thus appropriate to combine it with the C/R^3 correction. The total area of the tent is thus made to be

$$Q = (C/3)[(I_1/R_1^3) + (I_2/R_2^3) + (I_3/R_3^3)], \quad (6)$$

where the I's are the line intensities and the R's are the distances from the origin to the three corners of the triangle.

Powder pattern computation

The procedure for computing a powder spectrum is as follows: a value for N, the number of intersections of the triangular grid along an edge of the octahedron, adequate to achieve the required accuracy is selected. The frequency and intensity of the line in the single crystal spectrum with the magnetic field oriented in the direction corresponding to a triangular grid intersection are calculated. The frequency is stored in an array indexed by integers i and j. The intensity is further corrected by the $1/R^3$ solid angle factor and then stored in a similar array. This calculation is repeated for every intersection in the grids covering the four faces of the octahedron for which $z \geqslant 0$. Some intersections in the $z = 0$ plane are diametrically opposed to others. Since the result does not depend on the sign of the magnetic field, frequencies and intensities for these pairs of intersections need be calculated only once. It can be shown that $2N^2 + 1$ calculations are required. Next the frequency range over which the spectrum is to be calculated and the number of discrete points into which this range is to be divided are selected. The contributions to the spectrum from each of the $4N^2$ triangles are then calculated with the two-dimensional interpolation method. The total intensity of the contribution from each triangle is approximated by averaging the solid angle corrected intensities at the three corners of each triangle. Equations (1a)–(1j) are used to add the proper value to each discrete point of the spectrum whose interval contains part of the tent from each triangle. The process is repeated for each line in the single crystal spectrum.

Figure 4(a) shows the result of such a powder pattern calculation for a single nucleus subject to an asymmetric chemical shift tensor. In this example N was 32 so that each face of the octahedron was partitioned into 1024 triangles, which requires that line frequencies and intensities at a total of 2049 magnetic field directions be calculated. Figure 4(b) shows the same powder pattern calculated with $N = 128$, requiring 32 769 magnetic field directions. The slight imperfections which are visible at the lower and upper edges of the pattern in the $N = 32$ spectrum are no longer present in the $N = 128$ spectrum. Figure 4(c) shows the same powder pattern calculated without interpolation, and by partitioning all directions with 1° increments in the polar and azimuthal angles, so that 64 621 magnetic field directions are required. In fact the deficiencies of this last spectrum are not as severe as they appear, because the "noise" is all of the sort which is well smoothed by convolution broadening.

Because this technique employs interpolation, the frequency as a function of magnetic field position relation must be smooth. In particular, for linear interpolation to be correct, a function must have continuous first derivatives. It would at first seem that this should always be the case, but subtle difficulties can arise. For example, the Pake doublet powder pattern shown in Fig. 5(a) was calculated by adding together patterns generated by the continuous functions $D[3\cos^2(\theta) - 1]/2$ and $-D[3\cos^2(\theta) - 1]/2$. The pattern in Fig. 5(b) was generated with the absolute value functions $|D[3\cos^2(\theta) - 1]/2|$ and $-|D[3\cos^2(\theta) - 1]/2|$, whose first derivatives are undefined at the magic angle where $\cos(\theta) = 1/\sqrt{3}$. The "glitch" in the center of the second spectrum is due to the failure of the interpolation at this point. This difficulty can arise inadvertently when Hamiltonian matrices are being diagonalized by numerical routines which sort the resultant eigenvalues in ascending order. When two eigenvalues cross, their identity is interchanged. If eigenvalues are identified by the order in which they appear rather than by the eigenvectors with which they are associated, the energy function will have a discontinuous first derivative and glitches will appear.

A listing of a program which implements the above algorithm in VAX/VMS FORTRAN-77 is available.

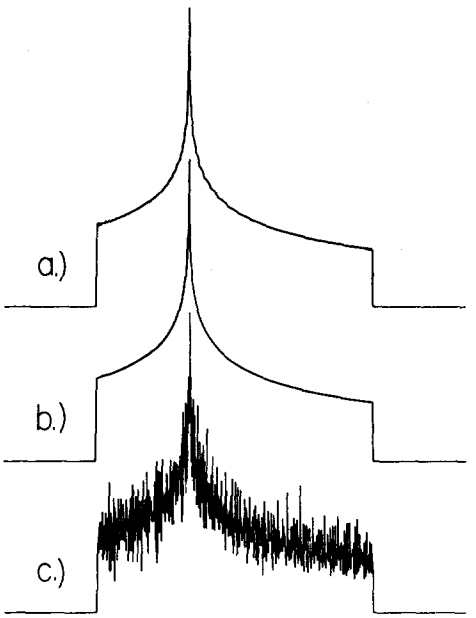

FIG. 4. Powder patterns calculated in 1024 frequency intervals. (a) Powder pattern calculated for asymmetric chemical shift tensor using two-dimensional interpolation and octahedral division of all directions. The edge of the octahedral face was divided into $N = 32$ segments, so that the frequency was calculated at 2049 magnetic field directions. (b) Same powder pattern with $N = 128$ requiring 32 769 calculations. (c) Same powder pattern calculated with no interpolation and using 1° increments in the polar angles θ and ϕ. The central peak is truncated to allow display on the same scale. 64 621 frequency calculations were required.

Convolution broadening

The calculated powder patterns of Figs. 4(a) and 4(b) have sharp discontinuities and peaks which are never observed experimentally because of broadening which invariably affects real spectra. It is thus necessary to broaden the

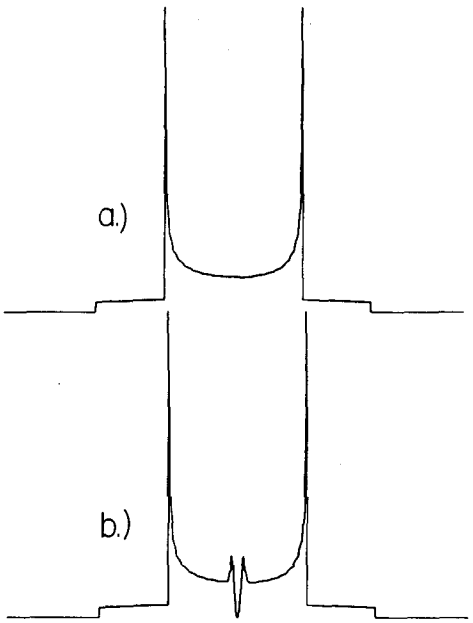

FIG. 5. (a) Pake doublet calculated with continuous functions $D[3\cos^2(\theta)-1]/2$ and $-D[3\cos^2(\theta)-1]/2$ and $N=32$. (b) Pake doublet calculated with absolute value functions $|D[3\cos^2(\theta)-1]/2|$ and $-|D[3\cos^2(\theta)-1]/2|$ and $N=32$. Distortion in the center of the spectrum is due to discontinuity of the derivatives of the absolute value functions.

theoretical spectra a like amount in order to fit the experimental data.

Such broadening is accomplished by convoluting the spectrum with a broadening function such as a Lorentzian or Gaussian line shape. It is well known that the most efficient way to compute a convolution of two functions is to Fourier transform the functions, multiply the two results together, and then inverse transform back to the original domain.[12] In the present case this involves starting out in the frequency domain, transforming to the time domain where the multiplication takes place, and then returning to the frequency domain with the inverse transform.

For a Lorentzian line shape with a full width at half-maximum w_L Hertz, the transformed time domain function is $\exp(-t\pi w_L)$. For a Gaussian line shape with a full width at half-maximum w_G Hertz, the transformed time domain function is $\exp(-t^2 w_G^2 \pi^2)/[4\ln(2)]$.

Because the powder pattern algorithm produces the absorption, but not the dispersion, part of the spectrum, some care is necessary in the application of the Fourier transform method to theoretical patterns. With the dispersion part of the spectrum zeroed the forward Fourier transform results in a symmetric time function. It is convenient, though not necessary, to preserve this symmetry so that the final result after the inverse transform is again only in the absorption. This is done by symmetrizing the Lorentzian and Gaussian transform functions in the time domain.

EXTRACTING NMR PARAMETERS

Least squares fitting

In least squares fitting a set of theoretical points is produced by calculation from a set of adjustable parameters and compared to the corresponding set of experimental points.[13] The parameters are then varied until the sum of the squares of deviations between the theoretical and experimental points is minimized. A brief summary of the pertinent statistical concepts of least squares fitting and error analysis is given in the Appendix.

In this work the data points are the discrete representation of the absorption spectrum and the theoretical parameters are such variables as chemical shift tensor elements and dipole–dipole coupling strengths.

To fit a powder spectrum the experimental data is first obtained by Fourier transforming the free induction decay and phasing the resultant spectrum. No line broadening is applied so as not to correlate the noise in the experimental points.

Theoretical spectra over the same spectral width and with the same number of data points M are then generated with the powder pattern and convolution algorithms discussed above. Because the theoretical and experimental spectra will in general have different scales and base line offsets, the theoretical spectrum is normalized by multiplying it by A and adding B. The values of A and B can then be chosen so as to obtain the best fit to the experimental spectrum by the least squares criterion. The values determined for A and B are not so important as the resulting minimum sum of the squares of deviations S^2. Because of the simple form of the least squares expression this adjustment can be done analytically. By taking the partial derivatives of the sum of the squares with respect to A and B and setting the two results to zero, solving the resultant equations for A and B, and inserting the results back into the equation for the sum of squares, it can be shown that the minimum sum of squares is given by

$$S^2 = \frac{M\Sigma e^2\Sigma f^2 - \Sigma e^2\Sigma f\Sigma f + 2\Sigma f\Sigma e\Sigma ef - M\Sigma ef\Sigma ef - \Sigma f^2\Sigma e\Sigma e}{M\Sigma f^2 - \Sigma f\Sigma f}. \tag{7}$$

The sums are over the M points in the spectra, the e are the experimental data points, and the f are the theoretical points. Care must be taken to avoid round-off errors during the numerical evaluation of this expression.

To find the best estimates of the spectrum parameters it is necessary to compute many theoretical powder patterns and find the values which minimize the sum of the squares given by Eq. (7). This is the classic nonlinear multiparameter minimization problem for which a number of strategies are available. In this work the Simplex method[9,14] has

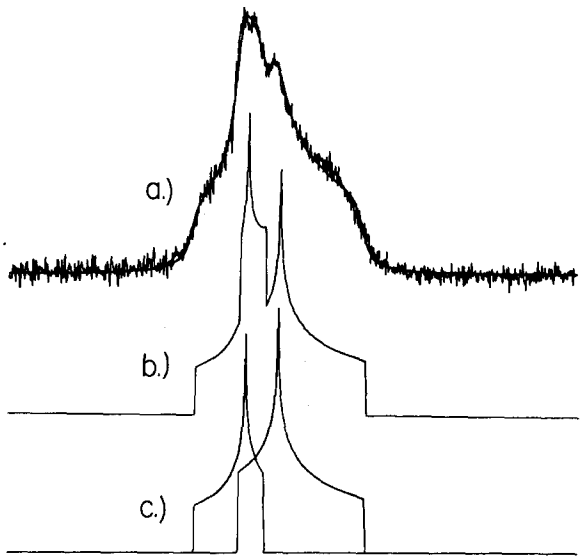

FIG. 6. (a) Theoretical fit and experimental 20.12 MHz carbon-13 spectrum of dimethoxymethane at 25 K, taken with a 50 KHz proton decoupling and 3 ms cross polarization time. There are 1024 points in the both spectra. No line broadening was applied to the experimental spectrum. (b) Sum of unbroadened powder patterns from chemical shift tensor values used to fit experimental spectrum of *a*. (c) Individual powder patterns.

been employed. As is always the case in multiparameter minimization, care must be taken to avoid interpreting a local, or "false," minimum as the global minimum.

EXAMPLE

Figure 6(a) shows a carbon-13 spectrum of dimethoxymethane, $CH_2(OCH_3)_2$, fit with two superimposed anisotropic chemical shift powder patterns, one for the methylene carbon and a second for the two methoxy methyl carbons. Ten parameters were used: the three principal values of the chemical shift tensor for the methylene carbon (δ^a_{11}, δ^a_{22}, and δ^a_{33}), the three principal values of the chemical shift tensor for the methyl carbons (δ^b_{11}, δ^b_{22}, and δ^b_{33}), the full widths at half-height of Lorentzian broadening functions for both the methylene and methyl carbons (w^a_L and w^b_L), and the scale and shift parameters A and B. The 2 to 1 ratio between the methyl and methylene line intensities was fixed. Only Lorentzian broadening was used in this dimethoxymethane fit. Another fit which included both Lorentzian and Gaussian broadening did not produce a significantly smaller sum of the squares of deviations, indicating that in this case Gaussian broadening is unnecessary.

The estimates for these parameters and the marginal standard deviations of the estimates, determined by the method described in the Appendix, are given in Table I. Figure 6(c) shows the two derived powder patterns, and Fig. 6(b) their sum, plotted without any line broadening.

The farthest upfield of the methyl principal values, $\delta^b_{33} = 9.12$ ppm, and the farthest downfield of the methylene principal values, $\delta^a_{11} = 128.73$ ppm, are well separated from any others, and are thus accurately determined with marginal standard deviations of 0.34 and 0.43 ppm, respectively. The central principal value for the methyl carbon, $\delta^b_{22} = 69.92$ ppm, is responsible for the prominent peak on the upfield slope of the experimental spectrum, and is particularly well determined with a marginal standard deviation of 0.28 ppm. The remaining principal values, $\delta^a_{22} = 92.62$ ppm, $\delta^a_{33} = 79.70$ ppm, and $\delta^b_{11} = 97.84$ ppm, all lie under the broad peak. The fitting procedure thus has greater difficulty fixing their values, and this difficulty is reflected in their larger marginal standard deviations of 0.52, 0.46, and 0.53 ppm, respectively. As is pointed out in the Appendix, these marginal standard deviations are not confidence intervals.

The correlation coefficients for the fit are given in Table II. Of the correlation coefficients between the chemical shift principal values, only two, those between δ^b_{11} and δ^a_{22}, and between δ^b_{22} and δ^a_{33}, are larger than 0.5. These correlations reflect the fact that the fitting procedure can trade off these closely spaced values without significantly degrading the fit of the theoretical spectrum to the experimental data.

The values of the broadening parameters, w^a_L and w^b_L, are due to relaxation and, in this instance, to deficiency in the proton decoupling. More effective proton decoupling would permit chemical interpretation of the broadenings. It is unfortunate, but not surprising, that w^a_L correlates strongly with the chemical shift tensor elements whose values are similar, δ^a_{22}, δ^a_{33}, and δ^b_{11}.

The values of A and B are arbitrary scaling parameters and have no chemical significance.

SUMMARY

The efficient method for computing patterns developed here, and the least squares fitting technique which it makes practical, should enhance the value of NMR spectroscopy of powdered solids. Accurate analysis of simple powder spectra is now routine, and interpretation of powder specta which arise from complex Hamiltonians is now possible. The error estimates which arise from the least squares fits provide information essential to the interpretation of the measured values.

TABLE I. Least squares fit results for dimethoxymethane.

Parameter	Parameter value	Marginal standard deviation
Methylene		
δ^a_{11}	128.73 ppm	0.43 ppm
δ^a_{22}	92.62 ppm	0.46 ppm
δ^a_{33}	79.70 ppm	0.52 ppm
w^a_L	191.06 Hz	12.92 Hz
Methyl		
δ^b_{11}	97.84 ppm	0.53 ppm
δ^b_{22}	69.92 ppm	0.28 ppm
δ^b_{33}	9.12 ppm	0.34 ppm
w^b_L	181.65 Hz	7.65 Hz
A	3.94×10^{-2}	2.05×10^{-4}
B	-1.80×10^{-2}	1.10×10^{-3}

All chemical shifts referenced to liquid TMS

TABLE II. Correlation coefficient matrix from least squares fit results for dimethoxymethane.

	δ^a_{11}	δ^a_{22}	δ^a_{33}	w^a_L	δ^b_{11}	δ^b_{22}	δ^b_{33}	w^b_L	A	B
δ^a_{11}	...	−0.05	−0.17	+0.19	+0.17	−0.10	−0.02	+0.12	−0.07	+0.05
δ^a_{22}	−0.05	...	−0.24	+0.66	−0.71	+0.23	0.00	+0.18	+0.25	−0.16
δ^a_{33}	−0.17	−0.24	...	−0.56	−0.17	+0.58	+0.04	−0.06	−0.28	+0.18
w^a_L	+0.19	+0.66	−0.56	...	−0.52	−0.19	+0.01	+0.19	+0.47	−0.31
δ^b_{11}	+0.17	−0.71	−0.17	−0.52	...	−0.43	−0.05	+0.13	−0.08	+0.05
δ^b_{22}	−0.10	+0.23	+0.58	−0.19	−0.43	...	+0.04	−0.10	−0.10	+0.07
δ^b_{33}	−0.02	0.00	+0.04	+0.01	−0.05	+0.04	...	−0.22	+0.15	−0.10
w^b_L	+0.12	+0.18	−0.06	+0.19	+0.13	−0.10	−0.22	...	+0.55	−0.37
A	−0.07	+0.25	−0.28	+0.47	−0.08	−0.10	+0.15	+0.55	...	−0.66
B	+0.05	−0.16	+0.18	−0.31	+0.05	+0.07	−0.10	−0.37	−0.66	...

ACKNOWLEDGMENT

This work was supported by National Science Foundation Grant No. CHE-8310109.

APPENDIX: LEAST SQUARES ANALYSIS

The following treatment of linear least squares fitting and error analysis follows Hamilton.[13]

Consider a set of M quantities f_m, subject to observation perturbed by independent random errors with zero means and equal variances, which depend linearly on P parameters x_p via the equation

$$f_m = \sum_{p=1}^{P} A_{mp} x_p. \tag{A1}$$

Unbiased minimum variance estimates $\hat{x}_p$ for the correct values of the parameters x_{0p} can be obtained by choosing values of the x_p which minimize the sum of the squares of deviations:

$$S^2 = \sum_{m=1}^{M} (\hat{f}_m - e_m)^2, \tag{A2}$$

where the $\hat{f}_m$ are calculated from $\hat{x}_p$ with Eq. (A1) and the e_m are experimental observations of the f_m. The variance–covariance or moment matrix, defined as

$$M_{pq} = \langle (\hat{x}_p - x_{0p})(\hat{x}_q - x_{0q}) \rangle, \tag{A3}$$

where the angle brackets $\langle\ \rangle$ denote the expected value, is useful for determining the accuracy of the derived parameters. An unbiased minimum variance estimate of M_{pq} is given by

$$\hat{M}_{pq} = \frac{S^2}{M-P} \left(\sum_{m=1}^{M} A_{mp} A_{mq} \right)^{-1}. \tag{A4}$$

This matrix is called the "estimated moment matrix." The marginal standard deviation of the estimate $\hat{x}_p$ of the parameter x_p is given by

$$\sigma_p = \sqrt{\hat{M}_{pp}} \tag{A5}$$

and the correlation coefficient between $\hat{x}_p$ and $\hat{x}_q$ is given by

$$\rho_{pq} = \frac{\hat{M}_{pq}}{\sigma_p \sigma_q}. \tag{A6}$$

The present problem is not linear, but since a general nonlinear error analysis is not possible, it must be linearized with the expansion around $\hat{x}_p$:

$$f_m = \hat{f}_m + \sum_{p=1}^{P} \frac{\partial f_m}{\partial x_p} (x_p - \hat{x}_p). \tag{A7}$$

Now the partial derivatives $\partial f_m / \partial x_p$ can be associated with the matrix elements A_{mp}, and from Eq. (A4) an estimated moment matrix for the nonlinear problem is

$$\hat{M}'_{pq} = \frac{S^2}{M\text{-}P} \left(\sum_{m=1}^{M} \frac{\partial f_m}{\partial x_p} \frac{\partial f_m}{\partial x_q} \right)^{-1}. \tag{A8}$$

The partial derivatives can be approximated numerically as

$$\frac{\partial f_m}{\partial x_p} = \frac{f_m(x_p + \delta_p) - \hat{f}_m}{\delta_p}, \tag{A9}$$

where $f_m(x_p + \delta_p)$ is produced by evaluating the nonlinear equations for the f_m with all of the x_q equal to their estimated values $\hat{x}_q$, except for x_p which is set to $(\hat{x}_p + \delta_p)$. The value of δ_p for each x_p must be chosen small enough to remain within the linear region and yet large enough to minimize round-off error.

In multiparameter estimation, confidence intervals are multidimensional volumes whose shape is related to the estimated moment matrix and whose size is given by the F distribution.[13] When a number of parameters are fit, a 50% confidence interval is many standard deviations. Thus, because of the linearization of the problem, great care must be exercised in extracting standard deviations and confidence intervals from $\hat{M}'_{pq}$. The derived error estimates are reliable only if they are much smaller than the region in which the expansion of Eq. (A7) is valid.

Though the scale and shift factors A and B enter the least squares minimization process in a special way, they are nevertheless adjustable parameters of the fit and must be included in the error analysis.

[1] G. E. Pake, J. Chem. Phys. **16**, 327 (1948).
[2] A. Abragam, *The Principles of Magnetic Resonance* (Oxford University, Oxford, 1961), p. 216.
[3] A. Pines, M. G. Gibby, and J. S. Waugh, Chem. Phys. Lett. **15**, 373 (1972).
[4] M. Mehring, *Principles of High Resolution NMR in Solids* (Springer, New York, 1983).
[5] (a) H. W. Spiess, Chem. Phys. **6**, 217 (1974); (b) H. W. Spiess, R. Grosescu, and U. Haeberlen, *ibid.* **6**, 226 (1974).
[6] K. W. Zilm, R. T. Conlin, D. M. Grant, and J. Michl, J. Am. Chem. Soc. **102**, 6672 (1980).
[7] Y. Siderer and Z. Luz, J. Magn. Reson. **37**, 449 (1980).

[8]K. W. Zilm and D. M. Grant, J. Am. Chem. Soc. **103**, 2913 (1981).
[9]S. Ganapathy, V. P. Chacko, and R. G. Bryant, J. Magn. Reson. **57**, 239 (1984).
[10]J. G. Hexam, M. H. Frey, and S. J. Opella, J. Chem. Phys. **77**, 3847 (1982).
[11]D. L. VanderHart, H. S. Gutowsky, and T. C. Farrar, J. Am. Chem. Soc. **89**, 5056 (1967).
[12]R. N. Bracewell, *The Fourier Transform and its Applications* (McGraw–Hill, New York, 1978).
[13]W. C. Hamilton, *Statistics in Physical Science Estimation, Hypothesis Testing, and Least Squares* (Ronald, New York, 1964).
[14](a) S. L. Morgan and S. N. Deming, Anal. Chem. **46**, 1170 (1974); (b) S. N. Deming and S. L. Morgan, *ibid.* **45**, 278a (1973); (c) J. A. Nelder and R. Mead, Comput. J. **7**, 308 (1965).